Numerical Modeling of Internal Flow Aerodynamics
Part 2: Unsteady Flows

Jean-François Guéry
SNPE Propulsion
Centre de Recherche du Bouchet
F-91710 Vert-le-Petit
FRANCE

NOTATIONS

a	sound velocity (m/s) = $\sqrt{\gamma r T}$
f_{nL}	nth longitudinal acoustic mode (Hz) (= $\frac{na}{2L}$ in a closed duct assumption)
$\dot{m}_w$	mass flow rate per injecting surface unit (kg/m^2)
P	pressure (Pa)
q_m	total mass flow rate (kg/s)
R	port radius
r_b	burning rate (mm/s)
T	temperature of the flow (K)
T_f	propellant flame temperature (K)
u	unsteady mean velocity component in the x-longitudinal direction (m/s)
u_v	axial mean velocity (m/s)
v	unsteady mean velocity component in the y-lateral direction (m/s)
v_{inj}	wall injection velocity (m/s)
w	unsteady mean velocity component in the w-lateral direction (m/s)
x,y,z	co-ordinate system (m)
ρ	density (kg/m^3)
ρ_s	propellant density (kg/m^3)

Dimensionless Parameter

Re_c	Reynolds number: $\rho u_v D_c/\mu$, where D_c is a characteristic diameter of the SRM
Re_w	wall injection Reynolds number: $\rho v_w h_c/\mu$
γ	specific heat ratio

INTRODUCTION

It has been widely reported in the open literature that large segmented and axisymmetric Solid Rocket Motors (SRM) are subject to pressure oscillations caused by vortex shedding at annular restrictors or cavities in the grain, and acoustic feedback resulting from impingement of the vortices on the nozzle or other obstacles. If they are well suited for combustion instabilities studies in tactical rocket motors, acoustic balance methods have proven inefficient in predicting stability of large segmented rocket motors (e.g. Ariane 5 MPS and Titan IV SRMU).

Paper presented at the RTO/VKI Special Course on "Internal Aerodynamics in Solid Rocket Propulsion", held in Rhode-Saint-Genèse, Belgium, 27-31 May 2002, and published in RTO-EN-023.

Report Documentation Page

Form Approved
OMB No. 0704-0188

1. REPORT DATE	2. REPORT TYPE	3. DATES COVERED
00 JAN 2004	**N/A**	**-**

4. TITLE AND SUBTITLE	5a. CONTRACT NUMBER
Numerical Modeling of Internal Flow Aerodynamics Part 2: Unsteady Flows	5b. GRANT NUMBER
	5c. PROGRAM ELEMENT NUMBER
6. AUTHOR(S)	5d. PROJECT NUMBER
	5e. TASK NUMBER
	5f. WORK UNIT NUMBER
7. PERFORMING ORGANIZATION NAME(S) AND ADDRESS(ES) **SNPE Propulsion Centre de Recherche du Bouchet F-91710 Vert-le-Petit FRANCE**	8. PERFORMING ORGANIZATION REPORT NUMBER
9. SPONSORING/MONITORING AGENCY NAME(S) AND ADDRESS(ES)	10. SPONSOR/MONITOR'S ACRONYM(S)
	11. SPONSOR/MONITOR'S REPORT NUMBER(S)

12. DISTRIBUTION/AVAILABILITY STATEMENT
Approved for public release, distribution unlimited

13. SUPPLEMENTARY NOTES
See also ADM001656., The original document contains color images.

14. ABSTRACT

15. SUBJECT TERMS

16. SECURITY CLASSIFICATION OF:			17. LIMITATION OF ABSTRACT	18. NUMBER OF PAGES	19a. NAME OF RESPONSIBLE PERSON
a. REPORT	b. ABSTRACT	c. THIS PAGE			
unclassified	**unclassified**	**unclassified**	**UU**	**18**	

Standard Form 298 (Rev. 8-98)
Prescribed by ANSI Std Z39-18

For those situations, the full unsteady numerical simulation of the internal flow becomes the adequate solution. In general, simulations are done within two objectives:

- **Explanation**: this is the numerical simulation of a geometry defined at the time (web thickness) of maximum pressure oscillation after the firing of a SRM. This simulation will be generally made in a fixed geometry corresponding at that web thickness for a few acoustic periods. Frequencies and levels are expected from numerical simulation. The objective is to compute and explain the non linear coupling mechanisms between hydrodynamic instabilities and acoustics leading to such levels, with associated processes (conditions for resonance, aluminum combustion, fluid-structure coupling, ...).
- **Prediction**: in this simulation, we want to assess the effect of a change in SRM geometry, propellant, burning rate [1],... on thrust oscillations, before any firing. In that case, all the firing has to be examined since there is no way to determine a priori the time of maximum pressure oscillation.

The studies carried out in France during the last 10 years (POP and ASSM CNES programs) have displayed that vortex shedding due to annular restrictors is not the only process explaining the thrust oscillations of large SRM. It comes actually that pressure oscillations in large L/D ratio SRM could be due to three different vortex shedding phenomena [2]:

- Vortex shedding from annular restrictors,
- Vortex shedding over intersegment cavities,
- Surface vortex shedding [3].

This lecture will focus on some models used in CFD code for internal aerodynamics in SRM, validation cases, confrontations between experiments and simulations, and recent improvements.

GRAIN REGRESSION EFFECT

If we do not want to simulate the entire firing, but concentrate on a typical event (burst) some time during the firing, care must be taken for defining properly the computation initial conditions.

During the burning of a solid propellant grain, the internal geometry evolves continuously, leading to an evolution of the aerodynamic flow field and acoustic modes. When a hydrodynamic instability matches an acoustic mode, this slow evolution creates slow frequency changes, and waterfalls on successive acoustic modes.

We can define some characteristic times.

For the sake of simplicity, a global approach is given. In a SRM and in the steady state, pressure and temperature fields can be shown independent. We define $u_v(x)$ to be the axial mean velocity at an x axial position in the motor:

$$u_v = \frac{\dot{m}(x)}{\rho(x)A(x)}$$

with $\dot{m}(x)$ being the mass flow rate through the port cross area A(x) at abscissa x. This expression shows that this means velocity can vary for at least three reasons:

- a variation of the forward mass flow $\dot{m}(x)$
- a variation of the density (that is to say the mean pressure)
- a variation of the port cross area

Hence, four characteristic times can be defined:

1) $t_m = \dfrac{\dot{m}(x)}{\dfrac{d(\dot{m}(x))}{dt}}$

2) $t_p = \dfrac{P}{\dfrac{d(P)}{dt}}$

3) $t_b = \dfrac{R}{r_b}$

4) $t_u = \dfrac{u_v(x)}{\dfrac{d(u_v(x))}{dt}}$

The two first characteristic times can be any during some events in the burning (for instance when the burning surface reaches the structure).

The third characteristic time describes the slow evolution of the internal geometry.

The last characteristic time, related to the evolution of the mean velocity, can characterize constant Strouhal evolution rates.

Dimensionless parameters can be obtained through the product of these times with f_{1L}. For instance, in Ariane 5 SRM and in the last third of the firing, $t_b f_{1L}$ is around of 3000. It means that during 30 periods of the first acoustic mode, the port internal radius has varied of 1%.

These considerations show that in the majority of applications, the geometry can be considered fixed, defined by a ballistics restitution, when we want to compute the unsteady internal flow during a few first acoustic mode periods, and a way for verifying this hypothesis can be by computing these characteristic times.

PHYSICAL MODELS

In order to extend the credibility of numerical calculations as a predicting tool to be used for industrial applications either in development phases or in conceptual analysis phases, one needs to improve the level of accuracy of physical models and the effectiveness of numerical schemes. Numerical schemes are the "classical" ones used in CFD (generally, finite volume methods based on approximate Riemann solvers, with at least second order accuracy in space and time). Important physical models are two-phase and unsteady combustion models.

Unsteady Combustion Modeling

The pressure-coupled response links the fluctuations of the propellant injected specific mass flow rate to the fluctuations of the pressure, both being functions of the frequency through the pulsation $\omega=2\pi f$:

$$R_{mp}(\omega) = \frac{\dot{m}'/\overline{\dot{m}}}{p'/\overline{p}} \qquad (1)$$

This linear expression accounts for the coupling between unsteady combustion phenomena in the propellant and fluctuating pressure above the burning surface. The real part of the response indicates the portion of the mass burning rate which fluctuates in phase with the pressure, which means energy is exchanged between the pressure waves in the gas phase and the propellant burning surface. According to the sign of the real part of R_{mp}, pressure waves will be amplified ($\mathrm{Re}(R_{mp})>0$) or damped ($\mathrm{Re}(R_{mp})<0$) by the combustion. The analytical expression of the response can be deduced by modeling the heat flux transfer from the flame to the propellant surface and the heat diffusion inside the solid phase. Several non-linear models were proposed [20-22], and they usually differ one from the other in the expression of the instantaneous heat flux transmitted to the propellant.

Culick [21] has shown that all these models could lead to a same form for the linear response function, which is the two-parameter function:

$$R_{mp}(\omega) = \frac{nAB}{S + A/S - (1+A) + AB} \qquad (2)$$

where:

- n is the pressure exponent of the steady-state burning rate law $V_c = \alpha p^n$.
- A and B are non-dimensional parameters which characterize the propellant and depend on its physical and chemical properties. A is related to the pyrolysis kinematics and B to the energy released at the surface of the propellant.
- S is a Laplace variable, here defined by equation: $S(S - 1) = i\Omega$, where $\Omega = a\omega/V_c^2$, a being the propellant thermal diffusivity.

In an internal CFD code, the pressure-coupled response can be modeled through a detailed physical model, CPU time consuming, or in a very simpler way (Traineau et al.) [16]. The ONERA representation of the unsteady propellant combustion prescribes the instantaneous specific injected mass flow rate as:

$$\dot{m}(t) = \overline{\dot{m}} + \frac{\overline{\dot{m}}}{\overline{p}} \int_0^{t-t_0} R(\tau)\left[p(t-\tau) - \overline{p}\right] d\tau \qquad (3)$$

where $R(\tau)$ is the impulse response associated with propellant pressure-coupled response and quantities with an overbar are mean values.

Assuming the response function R_{mp} is known (i.e. the values of A and B are determined from experimental points) for a given frequency range [0-f_{max}], its associated impulse response can be deduced easily by applying an inverse Fourier Transform to R_{mp}. The time resolution of the impulse response function has to be adjusted according to the time step of the Navier-Stokes simulation.

The model implementation mainly consists in replacing the propellant boundary condition used in Navier-Stokes solvers (calculation of the injected mass flow rate from the steady-state burning rate law in αp^n) by a new boundary condition derived from equation (3). The injected specific mass flow rate is computed from Eq. (3) on each grid cell on the propellant surface, not necessarily for each time step dt since usually $d\tau$ is much greater than dt. One has to note that the use of this unsteady propellant combustion model implies the user has previously performed a reference computation with a steady-state burning rate, as expression (3) requires the estimate and storing of the means values of the pressure and injected mass flow rate, for each cell on the propellant burning surface.

Two-Phase Flows

Aluminized propellants give liquid aluminum oxide in the chamber. This two-phase-flow can significantly influence motor performance in terms of acoustic stability, slag accumulation, nozzle erosion, two-phase losses, and so on…

The internal unsteady two-phase flows can be solved with eulerian or lagrangian approaches and are described in the previous lecture [4].

The condensed phase can be considered inert or reactive. Most of aluminum combustion models are derived from Law's model [5].

TURBULENCE

Specific turbulence models must be used for studying unsteady flows in SRM. Usually, two kind of models are used: URANS and LES. These models must also take two-phase flow effects into account.

VALIDATION CASES

Many strategies can be used to validate multidimensional computations. The more logical one is to go from confrontations to simple 1D analytical results to full scale comparison with experiments.

Comparison to Analytical Results

Most of them are 1D theories. For instance, Morfouace and Tissier [6] have studied the acoustic wave damping of a two-phase flow in a duct in a very simple test case: the geometry in an open duct, a sinusoidal pressure signal is applied at the entrance, and a non reflecting boundary condition is used at the exit. They compared their results to Culick [7] and Temkin and Dobbins [8] theories.

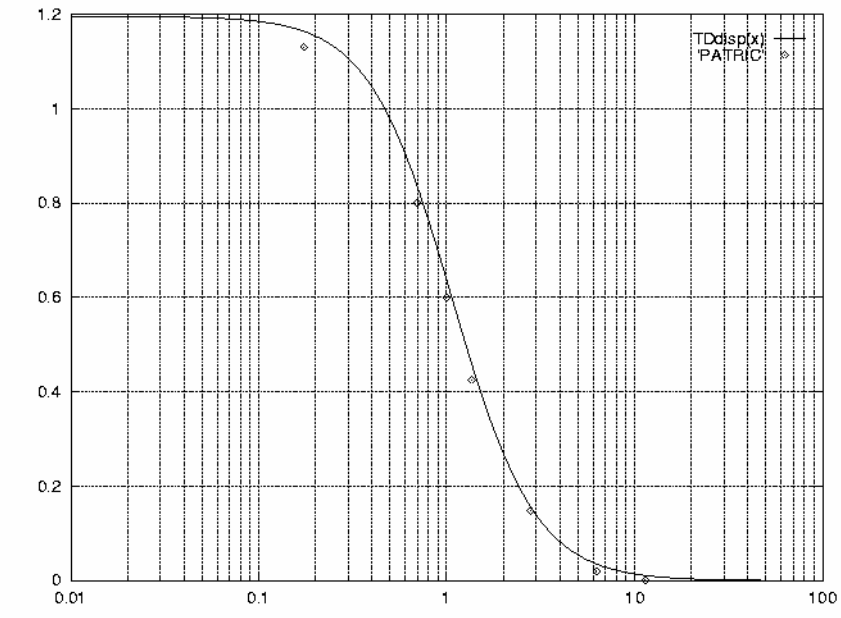

Figure 1: Comparison between 1D Computation (PATRIC) and TD Theory (Dispersion vs Dimensionless Frequency).

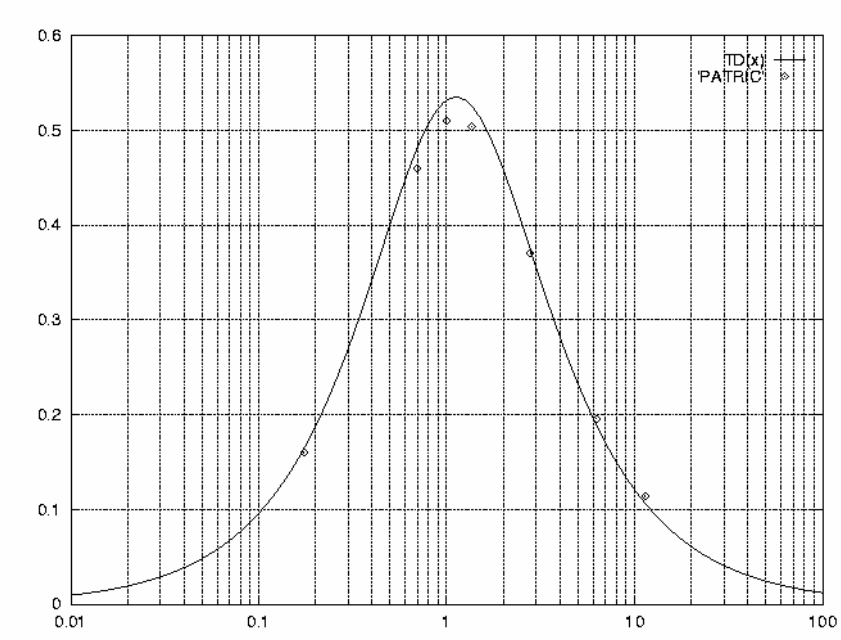

Figure 2: Comparison between 1D Computation (PATRIC) and TD Theory (Damping vs Dimensionless Frequency).

Comparison to Acoustic Balance

Vuillot et al. [9] have extended the validation to two-dimensional situation. In their paper, 2D Navier-Stokes stability computations are performed on a simple cylindrical port motor.

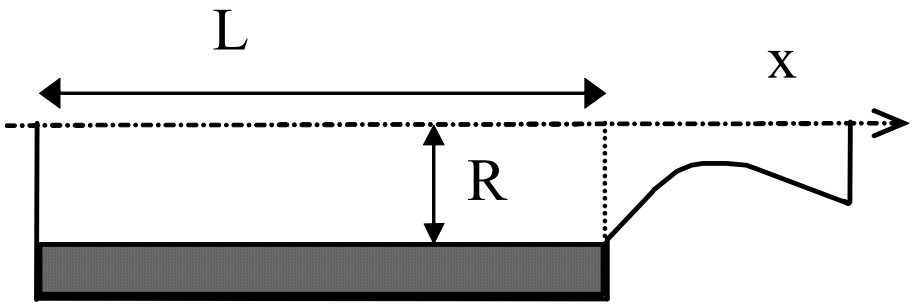

Figure 3: Schematic View of Vuillot et al. Test Case.

The 2D results, in terms of motor frequency and damping, as well as in terms of full acoustic field, are compared to classical 1D linear acoustic balance performed for the first longitudinal mode. The 2D computations are performed in the following way: after convergence toward a steady state solution, the motor is excited close to its first longitudinal mode by means of one period of head end forcing. Then the response of the flow field to that perturbation is analyzed, in term of frequency and exponential damping. The 2D computations are performed with models representing the propellant combustion response and two-phase flow behavior. The models are used separately and then together.

The results obtained for various model parameter settings as well as for various griddings are compared to linear results.

Noting Ω the interior of the chamber, $\partial\Omega$ its boundary, considering harmonic motions ($F'=\tilde{F}\exp(i\omega t)$) and using the following notations:

$$k_N=\frac{\omega_N}{a}$$

$$E_N^2=\int_\Omega \tilde{p}_N^2\,dV,\quad A_n=\bar{\rho}a\frac{\tilde{u}_i n'_i}{\tilde{p}},\quad M_n=\frac{\bar{u}_i n'_i}{a}$$

where n'_i is the inward pointing unit normal vector, the linear stability results are:

$$\omega-\omega_N=\frac{a}{2E_N^2}\int_{\partial\Omega} Im(A_n)\tilde{p}_N^2\,dS-\frac{a}{2k_N E_N^2}\int_\Omega Re\left(\delta\tilde{F}_{pi}\frac{\partial\tilde{p}_N}{\partial x_i}\right)dV+(\gamma-1)\frac{1}{2E_N^2}\int_\Omega Im\left(\delta\tilde{Q}_p\tilde{p}_N\right)dV$$

$$\alpha=\frac{-a}{2E_N^2}\int_{\partial\Omega}\left(Re_7(A_n)+\bar{M}_n\right)\tilde{p}_N^2\,dS-\frac{a}{2k_N E_N^2}\int_\Omega Im\left(\delta\tilde{F}_{pi}\frac{\partial\tilde{p}_N}{\partial x_i}\right)dV-(\gamma-1)\frac{1}{2E_N^2}\int_\Omega Re\left(\delta\tilde{Q}_p\tilde{p}_N\right)dV$$

The surface integral is usually split over the propellant surface (combustion driving, α_C) and the nozzle entrance plane (nozzle damping expressed as the sum of a convective part α_{NC} and a radiative part α_{NR}). It is a common use to add a so-called "flow-turning" damping term, α_{FT}, or to correct the propellant admittance for the displacement effect of the ABL (α_{BL}). The last two volume integrals are directly linked with the condensed phase and disappear for a one phase flow. δF and δQ are respectively the drag force exerted by the particles on the gas and the heat exchanged between the two phases. The overall expression for the resulting frequency shift and damping is:

$$\Delta\omega = \Delta\omega_C + \Delta\omega_{NR} + \Delta\omega_p$$

$$\alpha = \alpha_C + \alpha_{BL}\ (or\ \alpha_{FT}) + \alpha_{NC} + \alpha_{NR} + \alpha_p$$

The integral over the burning surface can be simplified by making use of the propellant pressure coupled combustion response, R_{MP}, defined as:

$$R_{MP}=\frac{v'_c/\bar{v}_c}{p'/\bar{p}}=\frac{\rho'/\bar{\rho}}{p'/\bar{p}}+\frac{\bar{p}}{aM_{inj}}\frac{u'_i.n'_i}{p'}$$

$$\Rightarrow R_{MP}=\frac{1}{\gamma M_{inj}}\left[M_{inj}+A_n\right]$$

so that: $\alpha_c=-\gamma a M_{inj}\,Re(R_{MP})\dfrac{\int_{S_{inj}}\tilde{p}_N^2\,dS}{2\int_\Omega\tilde{p}_N^2\,dV}$

For the simple cylindrical port, the damping take simplified expressions. The following relationships apply for this simple situation:

$$S_{inj}=2\pi RL,$$
$$S_L=\pi R^2,$$
$$\Omega=\pi R^2 L$$
$$M_L=\frac{S_{inj}}{S_L}M_{inj},$$
$$M_{inj}=\frac{V_{inj}}{a}$$
$$\tilde{p}_N=\tilde{p}_{N0}\cos(k_N x) \quad with \quad k_N=q\frac{\pi}{L}$$

leading to:

$$\alpha_c=-\gamma\frac{V_{inj}}{R}Re(R_{MP})$$

$$\alpha_{NC}=\frac{aM_L}{L}=\frac{2V_{inj}}{R}$$

$$\alpha_{NR}=\frac{aRe(A_L)}{L}$$

$$\alpha_{FT}=\alpha_{BL}=\frac{V_{inj}}{R}$$

$$\alpha_p=\kappa\frac{\omega}{2}\left[\frac{\omega\tau_v}{1+(\omega\tau_v)^2}+(\gamma-1)\frac{C}{C_p}\frac{\omega\tau_T}{1+(\omega\tau_T)^2}\right]$$

κ is the particle to gas mass ratio ($\kappa=C_m/(1-C_m)$, where C_m is the propellant particle loading). τ_u and τ_T are relaxation times given by $\tau_u=\frac{\rho_{material}D_p^2}{18\mu}$ and $\tau_T=\frac{3}{2}\Pr\frac{C}{Cp}\tau_u$ with *Pr,* the Prandtl number.

Comparison of linear acoustic balance and 2D computation on coarse and fine grids are given in Figure 4 and Figure 5.

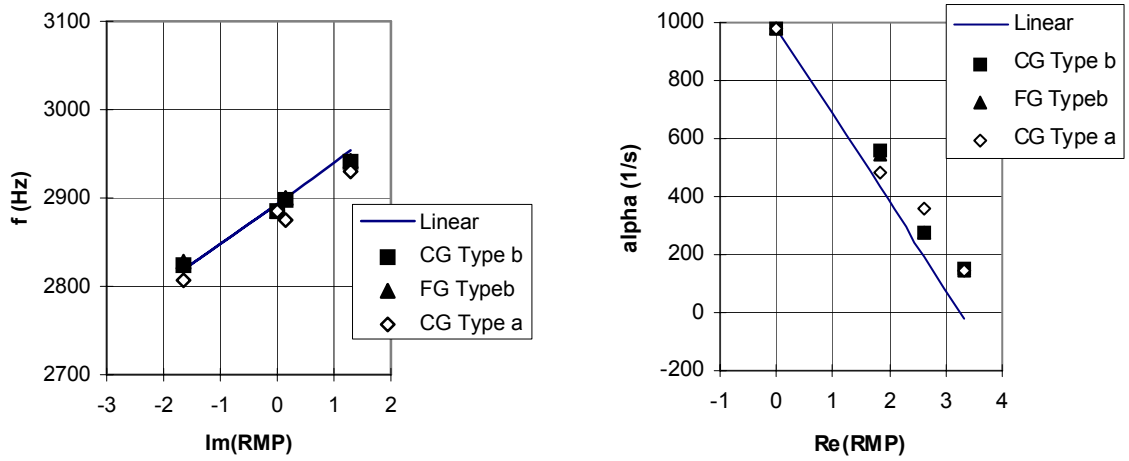

Figure 4: Summary of Computations with the Propellant Response Function Model (Coarse grid CG, fine grid FG, and two types of propellant response).

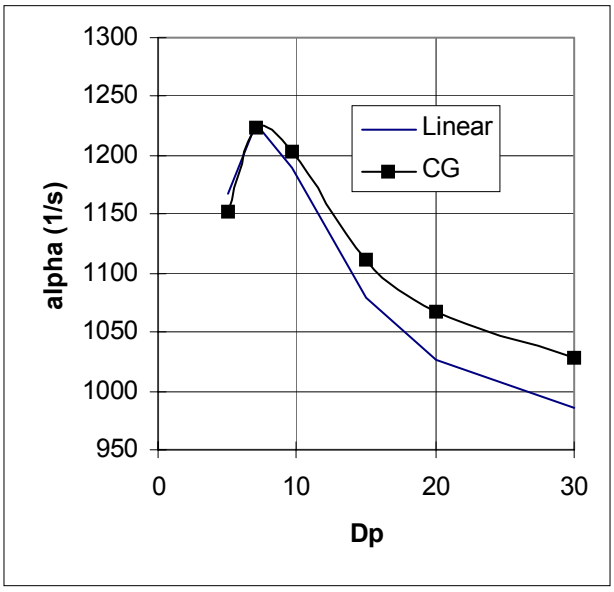

Figure 5: Particle Size Effect on Two-Phase Flow Damping.

The results show that the overall tendencies are correctly obtained over a large range of model parameter settings. Surprisingly it is found that the 2D results do not depend on the grid spatial resolution and that the details of the so-called acoustic boundary layer (ABL) do not need to be resolved.

This finding is also true for the two-phase flow damping. Analysis of the computed 2D acoustic field show that the ABL displacement effect is an effective damping source (even for an ABL penetrating into the core of the flow) and that an extra damping exists which is not incorporated into the classical acoustic balance.

Cold Flows

Since the internal flows in a solid-propellant rocket motor are difficult to instrument, cold flow experimental simulations are an alternative tool for a detailed aerodynamic effects understanding

(see Guéry et al [18]). The three different instability behaviours can be obtained. If absolute instabilities can be naturally computed by solving the Navier-Stokes equations, the surface vortex-shedding instability, as a convective instability, is more complex to obtain. Ugurtas [10] injects a gaussian noise with an amplitude of 0.4% v_{inj} to simulate the VECLA experiments. Apte and Yang [11] forces the head end with a pressure oscillation equal to 5% of the head-end mean pressure at imposed acoustic frequencies in order to analyse unsteady flow organisation in Hervat and Traineau [12] cold flow simulation of a nozzleless rocket motor.

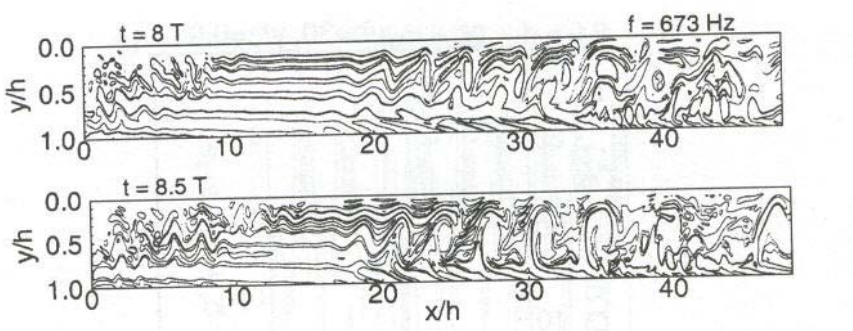

Figure 6: Eddy Motions in the Forced Acoustic Environment [11].

Validation on Simplified Rocket Motors

Dupays [13] developed a whistling motor (small and naturally unstable, based on VSA instability). He studied the effect of inert particulate phase in the propellant on the instabilities (vortex-shedding) by adding alumina or zirconium silicate particles in a AP/HTPB propellant. Different sizes and loading were used. Pressure oscillations were identified on all the firings, with some burst corresponding to self-sustained phenomena.

Experimental results are well reproduced by computations. When studying the particulate loading effect, with 5, 10 and 20 % of condensed phase, he noticed a curious effect: oscillations levels are larger with 10 % loading than 5 %, whereas 20 % loading damps out all the signal. These results are in contradiction with linear theory, and are not explained until now (particles/eddies interactions?).

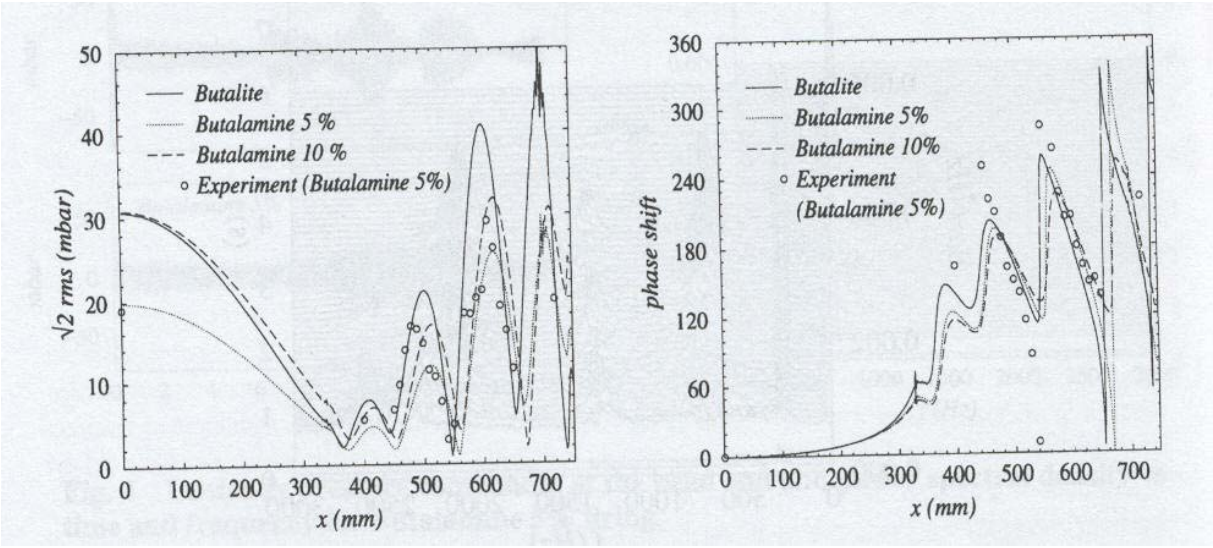

Figure 7: Comparison between Experiments and Computations (Dupays [13]).

RECENT IMPROVEMENTS

Full Motor Firing Simulation

The main project actually in the world leading to the detailed full numerical simulation of a SRM is the CSAR project at UIUC [14], and when GEN2 family codes (the last generation) will be operational, a large step in prediction will have been done.

SNPE developed the CPS and MOPTI® computer codes for CFD computations inside SRM. CPS solves the two and three dimensional compressible unsteady Navier-Stokes equations for turbulent, reactive, multi-species, two-phase flows with a cell-centered finite volume method on an unstructured mesh with triangular and quadrilateral control cells in 2D and with hexahedrons, pentahedrons, pyramids, prisms and tetrahedrons in 3D. It incorporates fluid-structure coupling facility, and is parallel. MOPTI® manages exchanges between two principal computational modules:

- A varying burning rate surface burnback module,
- CFD code CPS.

MOPTI® has been precisely described in reference [1]. The global structure of MOPTI is presented on Figure 8.

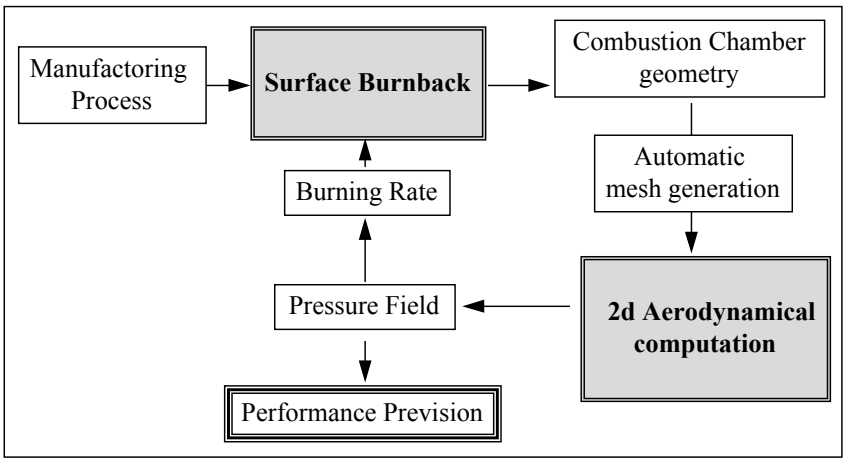

Figure 8: Structure of MOPTI®.

A MOPTI® simulation of the Ariane 5 1/15 subscale motor (LP6) is given [15]. On Figure 9 numerical vorticity fields are presented. They show that the flow becomes unstable after t≅5s. Before this time, the pressure signal is stable.

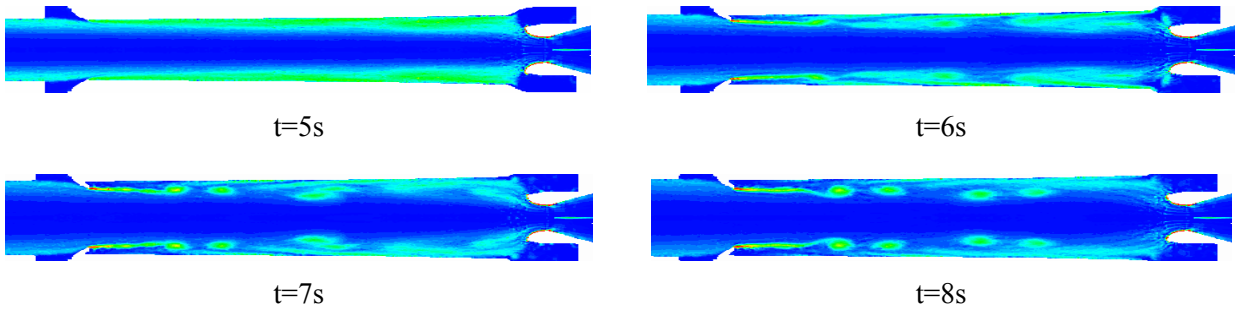

Figure 9: Numerical Vorticity Fields.

Those figures show a very good agreement between numerical and experimental results. The first oscillations occur after t≅5s. A first waterfall on the first longitudinal acoustic mode is observed between 5 an 6.5s. The levels are stronger on computational results but the global form is similar. The principal waterfall occurs between 6.5 and 8s, and a last one in the combustion tail off between 8 and 10s. For both waterfalls the numerical and experimental results are in really good agreement. The same comparison may be done on the second acoustic mode.

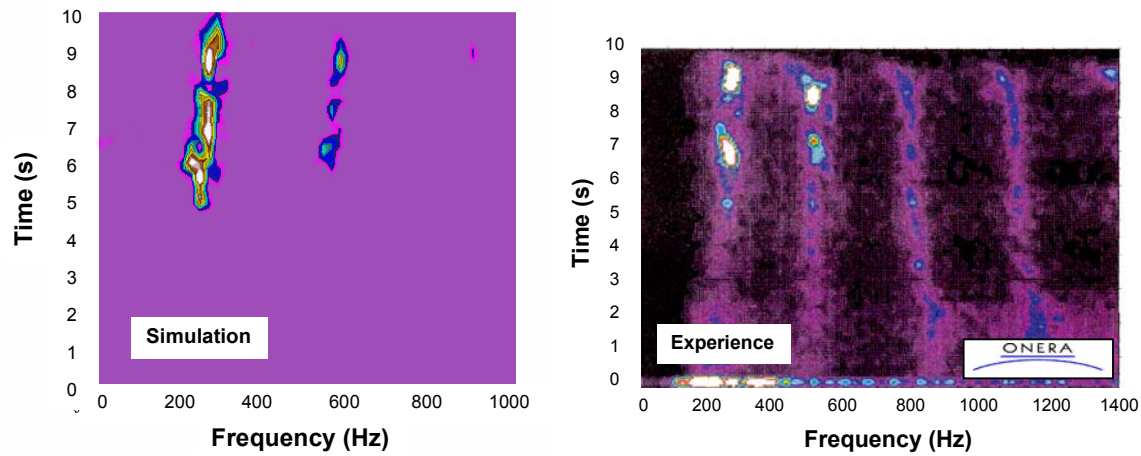

Figure 10: PSD Contours – Comparison of Experimental and Computational Results.

Fluid-Structure Coupling

In segmented motors with inhibited faces, a strong effect of the static bending of the emerging thermal inhibitors on pressure oscillation levels has been observed [16]. In order to investigate the influence of the dynamic behavior of the thermal inhibitor, CPS fluid-structure coupling facility has been used [17].

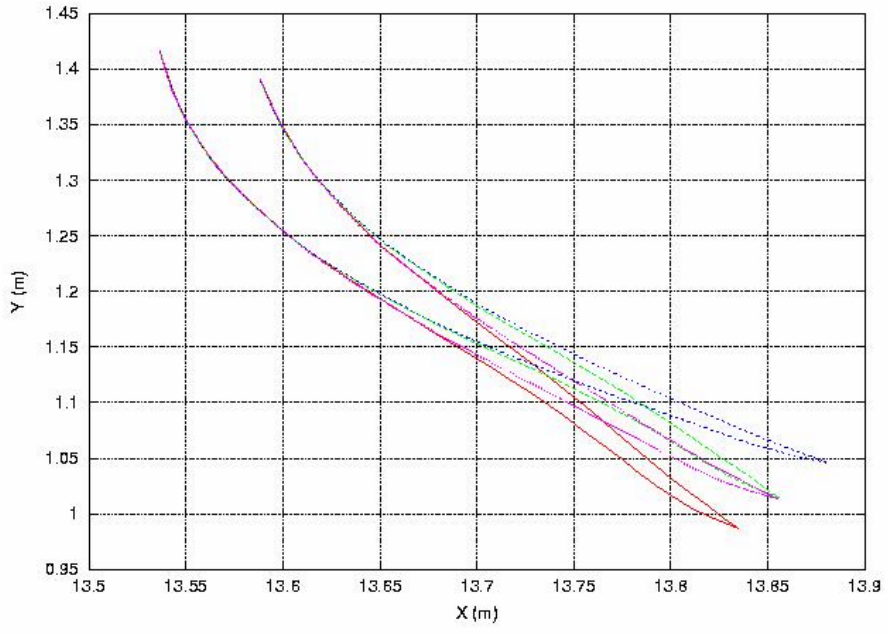

Figure 11: Deformed Shape of the Inhibitor at Different Times in the FSC Computation.

This computation is noted FSC. Unsteady pressure signal and its Fourier analysis is given in Figure 12. A strong influence of this phenomenon is found in this configuration since the fluctuation levels reach 3.5 times configuration without FSC.

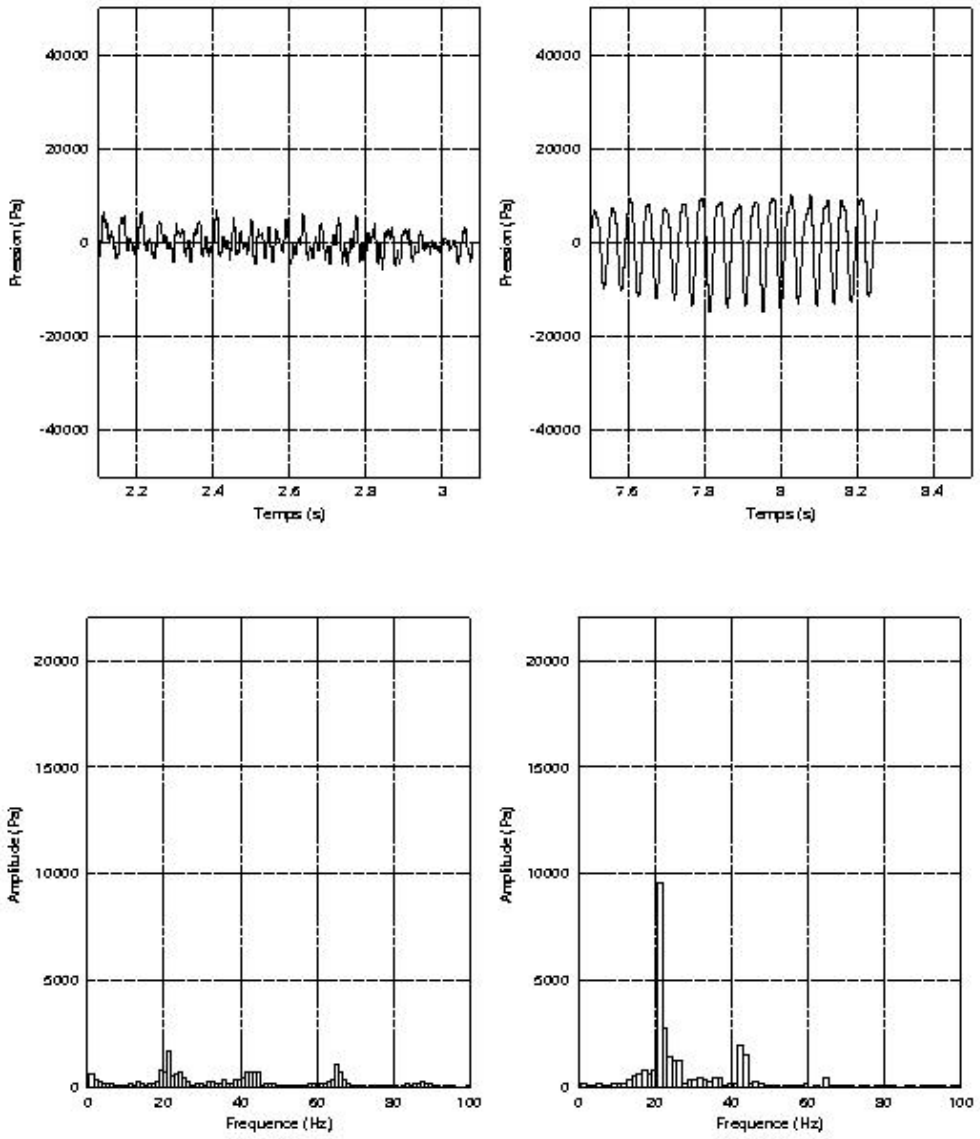

Figure 12: Head End Pressure Signal and its Fourier Transform.

This influence needs to be investigated in details. That could be done through cold flow experiments [18].

Effects of Aluminum Combustion

It is believed that aluminum distributed combustion and alumina droplets behavior might affect pressure oscillations of AP/Al propellant SRM, releasing heat inside the core of the flow. Such an eventuality has been assessed by using two-phase flow capabilities first at ONERA [15], then at SNPE [19]. A simplified combustion model has been used.

In these computations, Figure 13, particle distribution clearly displays vortex shedding and shows that momentum of particles are too large for their coming into vortex cores. The temperature map exhibits that combustion takes place very close to the surface and that some particles burn while passing round the vortices. Figure 14 presents pressure signals at the head end compared to the single phase computation in time and frequency space. It clearly points out a periodic signal and levels more than 4 times higher that those obtained with single phase computations.

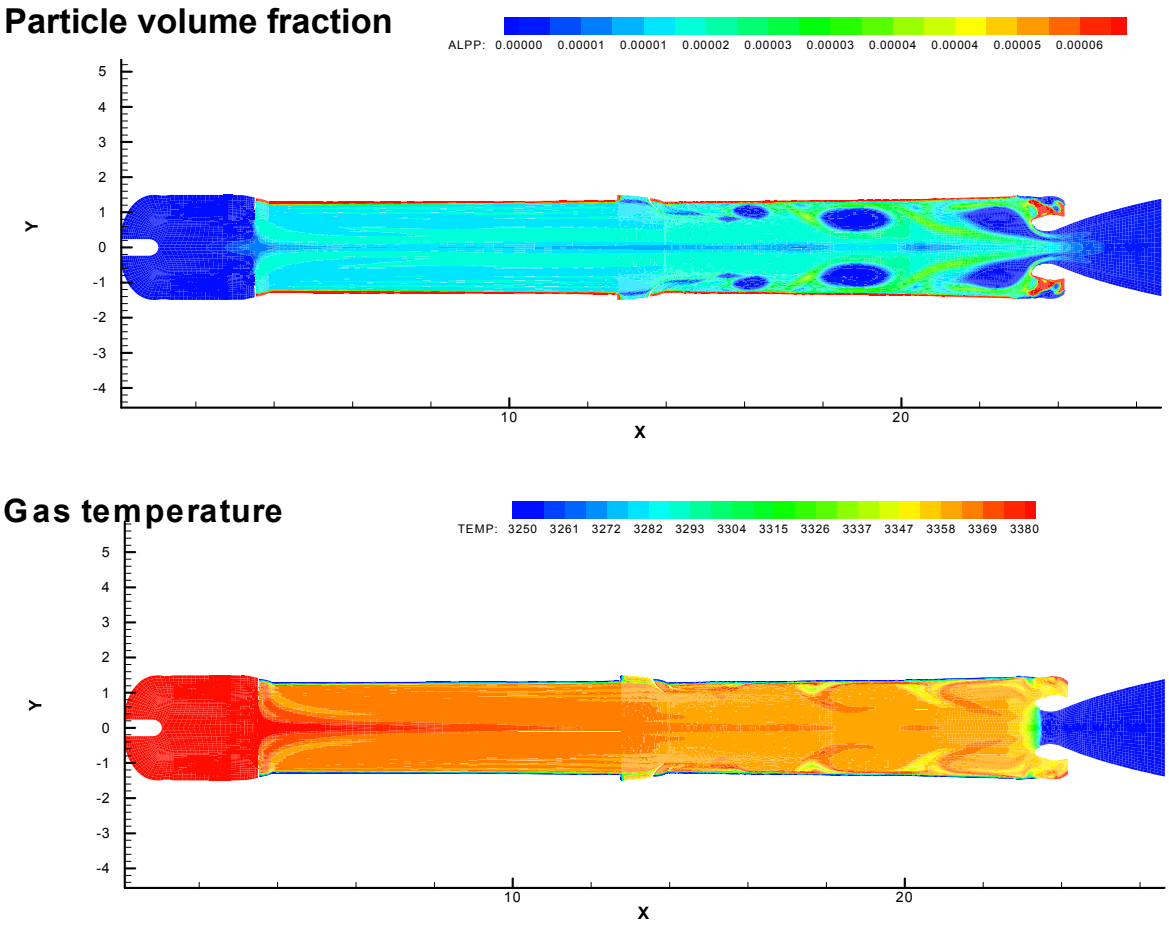

Figure 13: Particle Volume Fraction (up) and Gas Temperature (down).

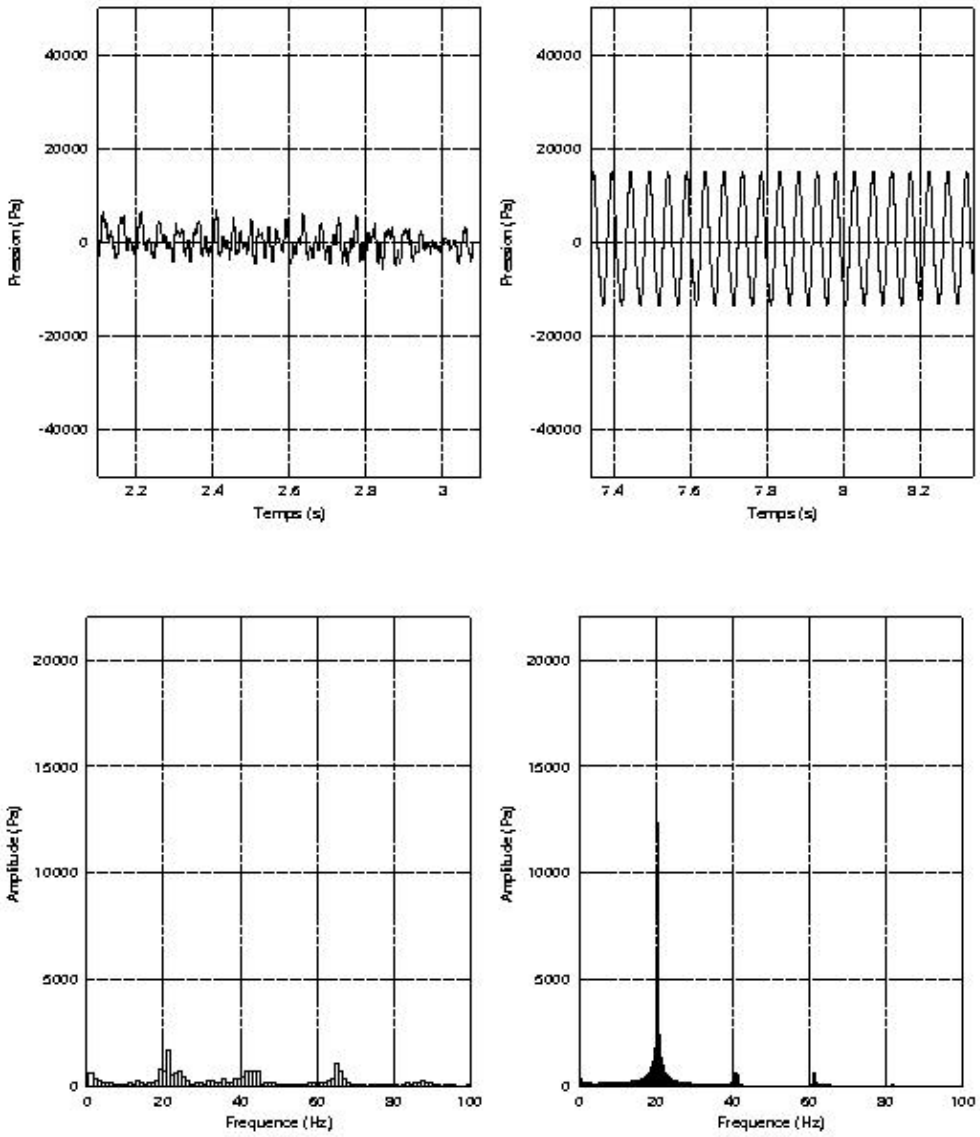

Bended inhibitor **Al Combustion**

Figure 14: Head End Pressure Signal and its Fourier Transform.

CONCLUDING REMARKS

Ten years after Kuentzmann [20] AGARD Lecture Series on combustion instabilities, we can measure the progress made in the numerical simulations of aerodynamic/acoustics coupling in SRM. This fantastic progress is due to two reasons. The first one is the continuously increasing performance of computers, giving scientists and engineers the opportunities for continuously increasing the accuracy of both numerical and physical models. But computer codes are nothing without validated models. The second reason has been the support of research programs in the US and France (ASSM and POP CNES programs for the French part).

During these ten years, numerical computation has gone from an academic research topic to an industrial powerful tool. And this was the second challenge for driving progress in SRM conception.

REFERENCES

[1] P. Le Breton, D. Ribéreau and F. Godfroy. "SRM Performance Analysis by Coupling Bidimensional Surface Burnback and Pressure Field Computations", AIAA 98-3968, July 1998.

[2] D. Ribéreau, J.-F. Guery and P. Le Breton, "Numerical Simulation of Thrust Oscillations of Ariane 5 Solid Rocket Boosters", Space Solid Propulsion, November 2000.

[3] N. Lupoglazoff and F. Vuillot, "Parietal Vortex Shedding as a Cause of Instability for Long Solid Propellant Motors. Numerical Simulations and Comparisons with Firing Tests", AIAA 96-0761, January 1996.

[4] J.F. Guéry, "Numerical Modeling of Internal Flow Aerodynamics", RTO-AVT-VKI Special Course, Internal Aerodynamics in Solid Rocket Propulsion, May 2002.

[5] C.K. Law, "A Simplified Theoretical Model for the Vapor-Phase Combustion of Metals Particles", Combustion Science and Technology, Vol. 7, N° 3-6, 1973.

[6] V. Morfouace and P.Y. Tissier, "Two-Phase Flow Analysis of Instabilities Driven by Vortex-Shedding in Solid Rocket Motors", AIAA 95-2733, July 1995.

[7] F.E.C. Culick, "Combustion Instability in Solid Rocket Motors", CPIA Publication 290, January 1981.

[8] S. Temkin and R.A. Dobbins, "Attenuation and Dispersion of Sound by Particulate-Relaxation Processes", J. of the Acoustical Society of America, Vol. 40, N° 2, 1966.

[9] F. Vuillot, J. Dupays, N. Lupoglazoff, Th. Basset and E. Daniel, "2D Navier-Stokes Stability Computations for Solid Rocket Motors: Rotational, Combustion and Two-Phase Flow Effects", AIAA 97-3326, July 1997.

[10] B. Ugurtas, G. Avalon, N. Lupoglazoff, F. Vuillot and G. Casalis, "Stability and Acoustic Resonance of Internal Flows Generated by Side Injection", in Solid Propellant Chemistry, Combustion and Motor Interior Ballistics, Progress in Astronautics and Aeronautics, Vol. 185, 2000.

[11] S. Apte and V. Yang, "Simulated Nozzleless Rocket Motor", in Solid Propellant Chemistry, Combustion and Motor Interior Ballistics, Progress in Astronautics and Aeronautics, Vol. 185, 2000.

[12] J.C. Traineau, P. Hervat and P. Kuentzmann, "Cold Flow Simulation of a Two-Dimensional Nozzleless Solid Rocket Motor", AIAA 86-1447, June 1986.

[13] J. Dupays, Y. Fabignon, P. Villedieu, G. Lavergne and J.L. Estivalezes, "Some Aspects of Two-Phase Flows in Solid Propellant Rocket Motors", in Solid Propellant Chemistry, Combustion and Motor Interior Ballistics, Progress in Astronautics and Aeronautics, Vol. 185, 2000.

[14] W.A. Dick, M.T. Heath and R.A. Fiedler, "Integrated 3D Simulations of Solid Propellant Rockets", AIAA 2001-3949, July 2001.

[15] P. Le Breton, J.F. Guéry, F. Vuillot and M. Prevost, "Recent Advances in the Prediction of SRM Thrust Oscillations", Colloque Vibration des Lanceurs, Toulouse, November 1999.

[16] J.C. Traineau, M. Prévost, F. Vuillot, P. Le Breton, J. Cuny and N. Preioni, "A Subscale Test Program to Assess the Vortex Shedding Driven Instabilities in Segmented Solid Rocket Motors", AIAA-973247, July 1997.

[17] P. Della Pieta et al, "Numerical Simulations of Some Fluid-Structure Interaction Phenomena Found in Solid Rocket Motors", paper to be submitted for publication to the Journal of Propulsion and Power.

[18] J.F. Guéry, F. Vuillot, G. Avalon, F. Plourde, J. Anthoine and B. Platet, "Use of Cold Flow Experiment in the ASSM Program: Lessons and Results" Space Solid Propulsion, Rome, November 2000.

[19] J.F. Guéry, S. Gallier, P. Della Pieta, F. Godfroy, A. Guichard, P. LeBreton and D. Ribéreau, "Numerical Simulation of Thrust Oscillations of Segmented AP/Al Solid Rocket Motors", IAF-01-S.2.05, October 2001.

[20] P. Kuentzmann, "Combustion Instabilities", AGARD-LS-180, 1991.